Research on Steel Surface Defects Detection Algorithms by YOLOv8 Based on Attention Mechanism

ShiQuan Gao, Ying Tian

***Abstract*—As deep learning advances, neural network technologies are increasingly penetrating the field of steel surface defect detection. To tackle the challenges of low accuracy and inadequate quality, we introduce CMS-YOLOv8s, a defect detection algorithm engineered for superior precision and efficiency. Initially, integrate the CBAM to enhance the network's focus on relevant information, allowing it to leverage multi-dimensional data like spatial and channel dimensions fully. Next, introduce the SPPFCSPC module to fuse feature information from different scales, expanding the model's receptive field and enhancing its feature extraction abilities. Finally, incorporate a small object detection head to boost the model's capability in identifying tiny targets, strengthening its ability to detect targets across different scales. Experimental findings show that CMS-YOLOv8s attains a detection accuracy of 70.4%, registering a significant 3.3% enhancement compared to the original YOLOv8s. This advancement distinctly improves defect detection accuracy across all categories.**

***Index Terms*—steel defect detection, YOLOv8s, CBAM attention mechanism, SPPFCSPC**

I. INTRODUCTION

During the processing of steel, factors like processing techniques and environmental uncertainties can give rise to surface defects for examples: cracks, patches, or scratches. Which not only diminishes the service life of the steel but also compromises its overall quality, posing potential safety hazards in various applications. Hence, attaining a high level of precision in detecting surface defects in steel is not only crucial but holds paramount significance [1-6].

Traditional defect detection methods predominantly involve manual inspection, leading to issues like low accuracy and slow efficiency. With the evolution of deep neural networks, defect detection has seen widespread application of deep learning-based object detection [7]. The primary detection algorithms can be categorized into two-stage detection models, represented by Faster R-CNN [8][24], and single-stage detection models, represented by YOLO[9] and SSD.

Although two-stage object detection algorithms deliver high detection accuracy, their methodology of initially generating candidate boxes and subsequently classifying them not only diminishes detection speed and efficiency but also escalates the computational burden on the model. In single-stage object detection algorithms, target detection is conducted during the forward propagation task without the necessity to generate candidate regions. These models predict the position and category of the target through anchor boxes, enabling faster inference speeds [9].The YOLO series detection algorithms are widely embraced in defect detection due to their simplicity, efficiency, and rapid detection capabilities [11][12][23].

At present, many domestic and foreign scholars have conducted a series of studies on steel defect detection. Reference [13] devised a fully convolutional YOLO network comprising 27 convolutional layers, producing a feature map with a size of 13×13. This improvement not only expands the receptive field for enhanced feature extraction but also strengthens the network's capability to detect small targets. In the YOLOv7 model, the introduction of the ECA by the reference [14] enhances the algorithm's feature learning capabilities, directing increased attention towards valuable information. In this study, the CBAM attention mechanism is integrated into the model. Which aims to improve the algorithm's feature learning abilities. It also reinforces the network's focus on spatial and channel aspects. Ultimately, this enhancement elevates the model's capacity for recognizing targets. Reference [15] made improvements to the neck module of YOLOv5 by introducing the BiFPN structure, a sophisticated cross-scale bidirectional fusion method. This innovation involves fusing features from various scales, thereby enhancing the model's capability to adapt to objects of various sizes. Reference [16] innovatively designed a new multi-scale block for image processing, leading to a notable improvement in the network's overall accuracy. Reference [17] adopted Partial Convolution as the foundational operator and introduced an improved Fusion module. This module not only preserves detection speed but also strengthens the feature extraction capabilities of shallow networks.

Summarizing the aforementioned, this paper proposes an enhanced method for detecting surface defects in steel, leveraging YOLOv8s. It integrates attention mechanisms to fine-tune the network's attention to relevant information and enhance feature extraction capabilities. The SPPFCSPC module extends the model's receptive field, fortifying its robustness, and improving the integration of features across varying scales. Adding a small object detection head significantly boosts the network's ability to identify tiny targets. This enhancement greatly improves precision in small

Manuscript received Feb 7, 2024; revised June 24, 2024.

Shiquan Gao is a postgraduate student of the School of Computer Science and Software Engineering, University of Science and Technology Liaoning, Anshan, 114051, China. (e-mail: 1441780082@qq.com)

Ying Tian is a professor at the School of Computer Science and Software Engineering, University of Science and Technology Liaoning, Anshan, 114051, China. (corresponding author to provide phone: +8613898015263; e-mail: astianying@126.com)

object detection, thereby enhancing the network's detection effectiveness.

II. RELATED WORK

The YOLOv8 algorithm represents the newest iteration in the YOLO series of one-stage target detection algorithms. It incorporates many SOTA technologies and boasts scalability. This encompasses various components such as the input module, the backbone network, the neck layer, and the head segment. Classified by depth and width, the network includes n, s, m, l, x, and so on five versions. The model parameters and computational load experience substantial increments with enhanced accuracy, meeting the demands of various scenarios [18].

The input module dynamically adapts the dimensions of input images through adaptive scaling and integrates mosaic data augmentation, thereby enhancing the model's performance.

The backbone network is made up of convolutional layers, C2f modules, and SPPF [19]. Multiple convolutional and C2f modules process input images to extract feature maps at diverse scales. The C2f module aims to provide comprehensive gradient flow information while keeping a lightweight design. Within the SPPF, feature fusion is achieved through a combination of pooling and convolution operations, enhancing the feature extraction ability of the model. The resulting features are then passed on to the neck layer.

The neck structure of YOLOv8 incorporates the FPN+PAN architecture [20], leveraging both top and bottom inter-layer connections to achieve feature fusion. This yields feature maps that integrate rich semantic information with precise localization details, ultimately improving the ability of the model to detect objects at different scales.

The Head utilizes a decoupled header structure, effectively segregating the detection from the classification tasks, and leverages the Task-Aligned Assigner for precise positive and negative sample matching. The loss computation encompasses both classification and regression aspects, employing binary cross-entropy as the classification loss[22]. Additionally, DFL and CIOU are introduced as regression losses to augment object detection.

III. IMPROVED MODULE

Fig. 1 illustrates the CMS-YOLOv8s network, which exhibits advanced improvements in object detection compared to YOLOv8s. Moreover, this model integrates the CBAM [21], SPPFCSPC module, and a dedicated layer for detecting small objects. These enhancements collectively elevate the model's detection capabilities, expediting convergence, expanding the model's receptive field, bolstering robustness, and optimizing both the efficiency and accuracy of the detection process.

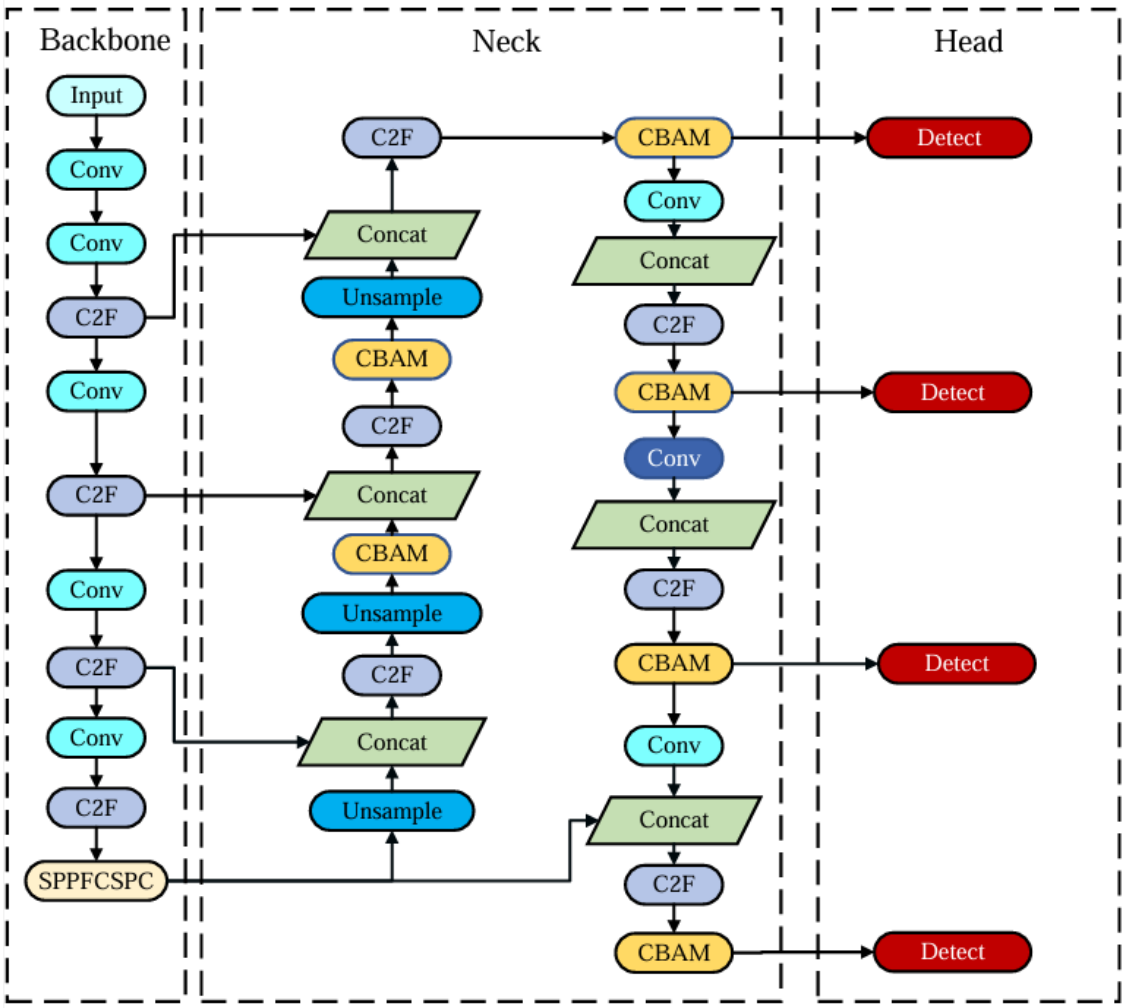

Fig. 1. CMS-YOLOv8s model

A. CBAM

CBAM (Convolutional Block Attention Module) stands as a lightweight attention mechanism, featuring two discrete sub-modules: Channel Attention Module (CAM) and Spatial Attention Module (SAM), which structure as shown in Fig. 2 These modules operate independently to apply attention to both channel and spatial. This paper adopts the CBAM to augment the model's feature expressiveness, emphasizing crucial features while suppressing unnecessary ones.

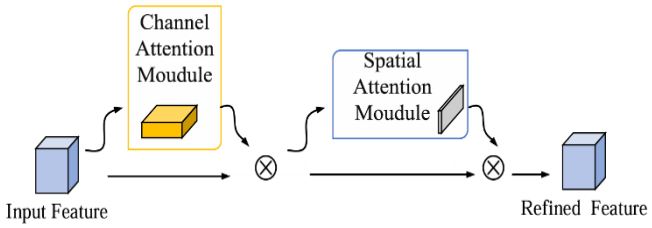

Fig. 2. Convolutional Block Attention Module

CAM operates on the input feature map F by applying global max pooling and global average pooling. The resulting feature maps are subsequently inputted into a two-layer neural network. The features outputted by the MLP are further subjected to summation, resulting in the generation of attention feature, denoted Mc. In this context, F^c_{avg} and F^c_{max} respectively represent average pooling and max pooling operations; σ shows the activation function; W_i signifies the weight matrix of perceptron layer i, and F represents the input feature map.Fig.3 illustrates the principle of CAM, and the calculation formula is as follows：

$$M_C(F)=\sigma\left(MLP\left(AvgPool(F)\right)+MLP\left(MaxPool(F)\right)\right)$$

$$=\sigma\left(W_1\left(W_0\left(F^c_{avg}\right)\right)+W_1\left(W_0\left(F^c_{max}\right)\right)\right) \quad (1)$$

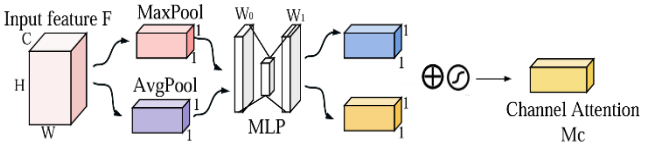

Fig. 3. Channel Attention Module

SAM takes F as the input, produced by channel attention. It then undergoes global max pooling and global average pooling along the channel dimension, resulting in two feature maps. These maps arefollowed by a 7×7 convolutional operation to generate the spatial attention feature, denoted as Ms. Ultimately, this characteristic is multiplied by the module's input feature to derive the final generated attribute. In this context: $f^{7\times7}$ represents the convolution operation. The corresponding model structure diagram and formula are as follows：

$$M_S(F)=\sigma\left(f^{7\times7}\left(\left[AvgPool(F);MaxPool(F)\right]\right)\right)$$

$$=\sigma\left(f^{7\times7}\left(\left[F^s_{avg};F^s_{max}\right]\right)\right) \quad (2)$$

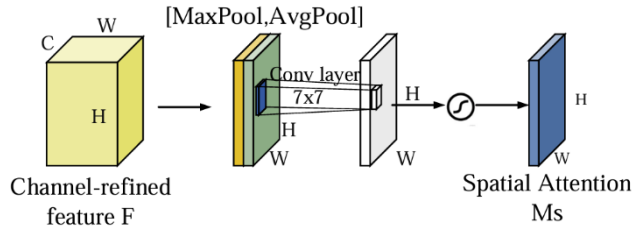

Fig. 4. Spatial Attention Module

B. Adding a small target detection head

The images examined in this paper depict surface defects in steel, utilizing the NEU-DET dataset, which contains numerous minuscule metal defects, with some having dimensions smaller than 10×10 pixels. The original YOLOv8 model undergoes five down-sampling stages, resulting in the loss of a substantial portion of feature information for these metal defects after multiple down-sampling steps. Despite employing an 80×80 detection head, detecting these types of metal defects at high resolution remains challenging.

In conclusion, to enhance the identification of minute metal defects, we integrated a novel 160×160 small target detection head into the model, as depicted in Fig. 5. This component encompasses more comprehensive underlying feature information of the targets, facilitating swift and efficient processing of small targets. Despite the increased computational demand attributed to adding the small target detection head, it markedly improves the efficacy in detecting and recognizing small targets.

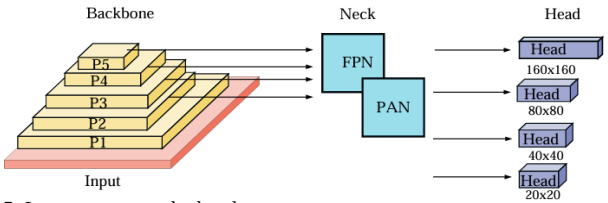

Fig. 5. Improvement at the head

C. SPPFCSPC

Spatial Pyramid Pooling (SPP) works by applying pooling at various scales to the feature map, yielding diverse pooling outcomes and acquiring different receptive fields. This design allows the model to effectively handle feature maps of varying resolutions. It adeptly mitigates challenges like image distortion resulting from operations such as scaling and cropping, addresses the model's tendency to repetitively extract image-related features, and enhances the speed of generating candidate boxes while concurrently reducing computational costs. The structural details are visually presented in Fig. 6.

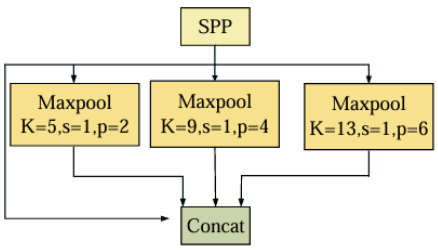

Fig. 6. Spatial Pyramid Pooling

The YOLOv5 algorithm undergoes enhancement by incorporating the Spatial Pyramid Pooling (SPP) structure, introducing the SPPF structure. This improvement entails repositioning the max-pooling layer within the architecture and adjusting parameters like convolutional kernel size, stride, padding, etc. These modifications are geared towards accelerating pooling speed while preserving the network's consistent receptive field size. The model is shown in the Fig. 7.

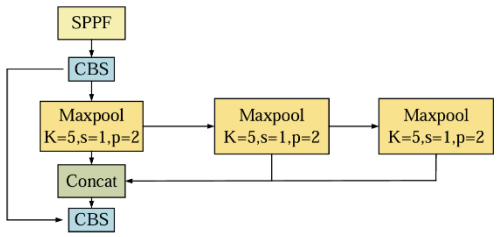

Fig. 7. Spatial Pyramid Pooling – Fast

In addition, the YOLOv7 algorithm proposes the SPPCSPC structure, building upon the Spatial Pyramid Pooling (SPP) architecture. Within the SPP, the Cross Stage Partial (CSP) structure is introduced, incorporating an additional residual branch. This augmentation serves to optimize input images, enhance feature extraction, and improve overall accuracy. The SPPCSPC structure is shown in Fig. 8.

Due to the introduction of the CSP structure in SPPCSPC, both model parameters and computational load increase, resulting in slower pooling speeds. To address this, building upon the SPPF concept, we propose an enhanced module termed SPPFCSPC. By adjusting the pooling kernel of the max-pooling layer, we aim to boost detection speed while maintaining detection effectiveness.

The SPPFCSPC module initially employs three CBS modules for image feature extraction. It then utilizes three distinct max-pooling layers to capture different-scale receptive fields, thus gathering more comprehensive feature information. Furthermore, by integrating two CBS modules with residual connections, the module achieves a more refined feature fusion, enriching the overall feature representation. The improved structure is shown in the Fig. 9.

IV. Experiment And Analysis

A. Datasets

This paper utilizes the publicly available Northeastern University Surface Defects Dataset (NEU-DET) for steel strip surfaces, which encompasses six primary types of defects. As illustrated in Fig. 10, these defects are labeled as follows: 0 for crazing, 1 for inclusion, 2 for patches, 3 for pitted surface, 4 for roll-in scale, and 5 for scratches. Each defect category comprises 300 images, totaling 1800 images across all categories. The dataset is randomly partitioned into training, validation, and test sets in a ratio of 7:2:1. In total, there are 1260 images in the training set, 360 in the test set, and 180 in the validation set.

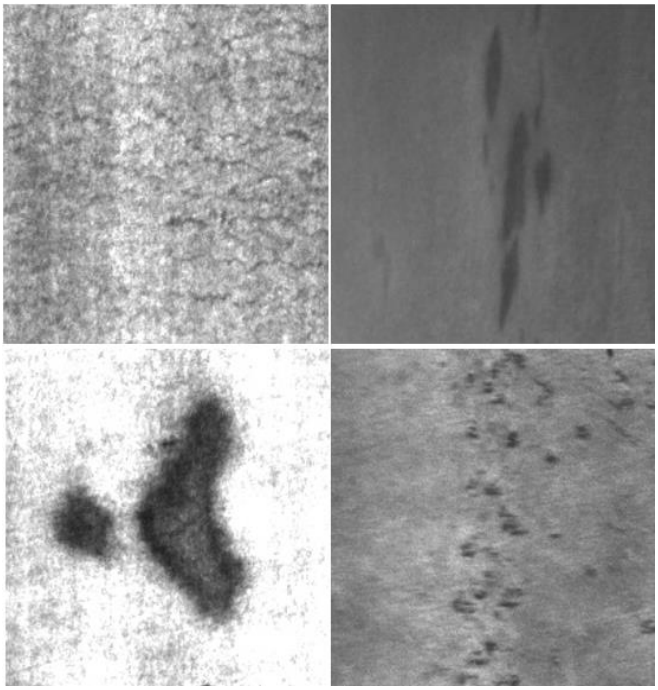

Fig. 10. NEU-DET Dataset

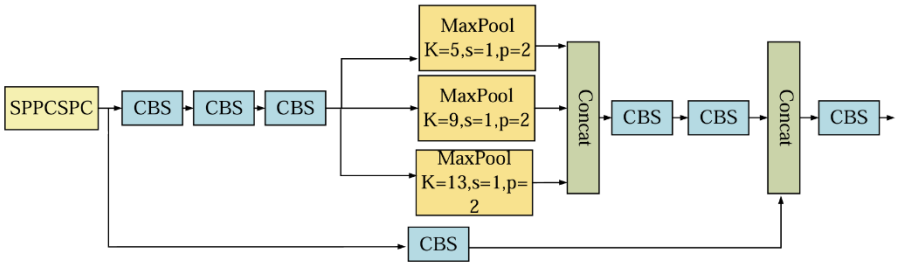

Fig. 8. SPPCSPC Model

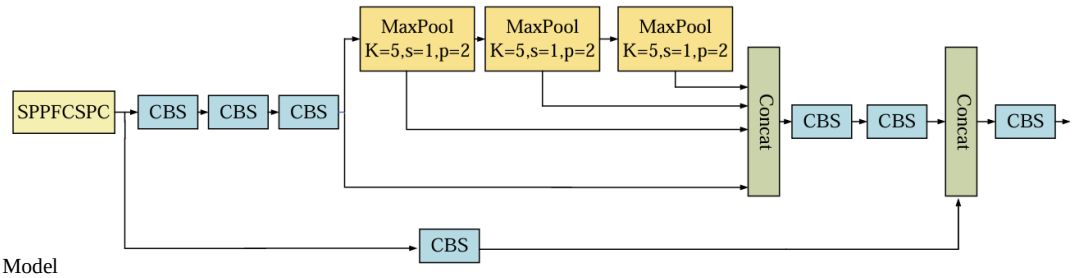

Fig. 9. SPPFCSPC Model

B. Evaluation Index

The experimental results in this paper utilize common evaluation metrics for object detection: Precision (P), Recall (R), and Mean Average Precision (mAP). The calculation formulas for these metrics are as follows:

$$P = \frac{TP}{TP+FP} \tag{3}$$

$$R = \frac{TP}{TP+FN} \tag{4}$$

$$mAP = \frac{1}{N}\sum_{i=1}^{N} AP_i \tag{5}$$

TP (True Positive) represents instances where the target in the image is correctly identified. FP (False Positive) refers to cases where the model correctly identifies the location of the target but misclassifies its category. FN (False Negative) indicates instances where the correct target is not identified and is considered as another object, leading to a missed detection. N represents the number of classes. A larger API area signifies a more effective classifier. mAP is the average of APi values across multiple classes. Additionally, to highlight the model's advantages on small devices compared to other models, we incorporate parameters such as model size, computation, and model file size as additional evaluation criteria.

C. Experimental Configuration

The experiment used the Ubuntu 22.04 operating system, Python as the programming language, and the PyTorch deep learning framework, version 1.8.1. The hardware includes a GeForce GTX 1080ti graphics card with 11178MB of memory. During the training process, the input image is adjusted to a size of 640×640, and Stochastic Gradient Boosting (SGB) is used as the optimizer function. The model was trained for 300 epochs with a batch size set to 1. The momentum and attenuation parameters are set to 0.937 and 0.0005 respectively, the learning rate is 0.01, and the cosine annealing scheduling algorithm is used. The Mosaic enhancement technique was used in the last 10 epochs of the training.

D. Experimental Results

Fig. 11 depicts the PR curves for YOLOv8s and CMS-YOLOv8s during testing on the NEU-DET dataset. The blue line represents the mAP curve at IoU 0.5, with precise values detailed in the accompanying table. Figure 11(a) displays the Precision-Recall (P-R) curve for the original YOLOv8s algorithm, while Figure 11(b) showcases the P-R curve for the enhanced CMS-YOLOv8s algorithm. In Figure 11(a), the area under the blue curve for mAP@0.5 is 67.1%, whereas in Figure 11(b), it reaches 70.4%. A larger area under the curve signifies superior model performance. The area under the blue curve in Figure 11(a) is smaller compared to the area in Figure 11(b), providing strong evidence for the effectiveness of the improved YOLOv8s algorithm in this study.

The numerical results and table highlight that the enhanced model exhibits accelerated convergence and substantial advancements in recognizing the majority of classes. Notably, significant improvements are observed in identifying defect categories like crazing, scratches, and patches, providing strong supporting evidence for the effectiveness of the proposed enhancement measures.

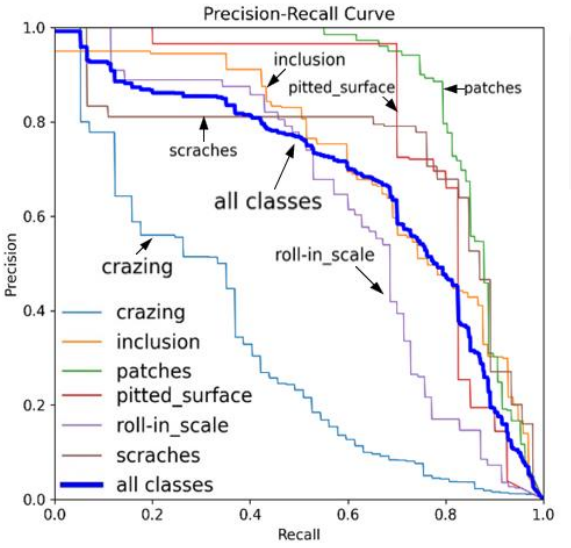

(a) YOLOv8s

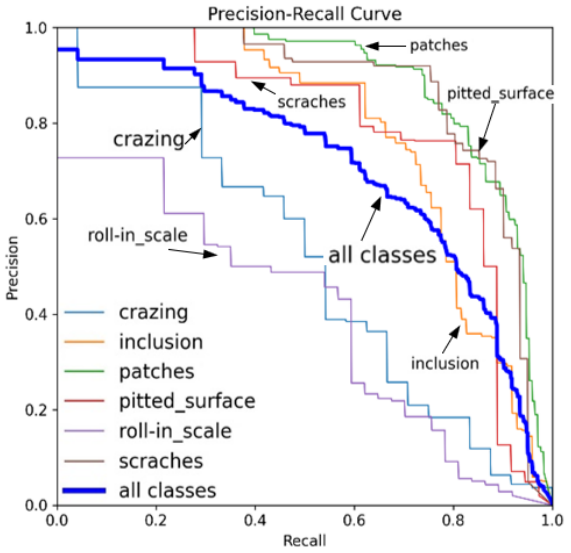

(b) CMS-YOLOv8s

Fig. 11. P-R curve on the NEU-DET dataset

TABLE I
THE P-R CURVES RESULTS ON NEU-DET DATASET

Class	YOLOv8s	CMS-YOLOv8s
Crazing	0.318	0.513
Inclusion	0.715	0.774
Patches	0.861	0.883
Pitted_surface	0.790	0.785
Roll-in_scale	0.616	0.601
scratches	0.728	0.867

E. Compare Test Results

Fig. 12 presents a comparative analysis of test results on the NEU-CET dataset. Three images were carefully chosen for this comparison: the top image is the test results of the

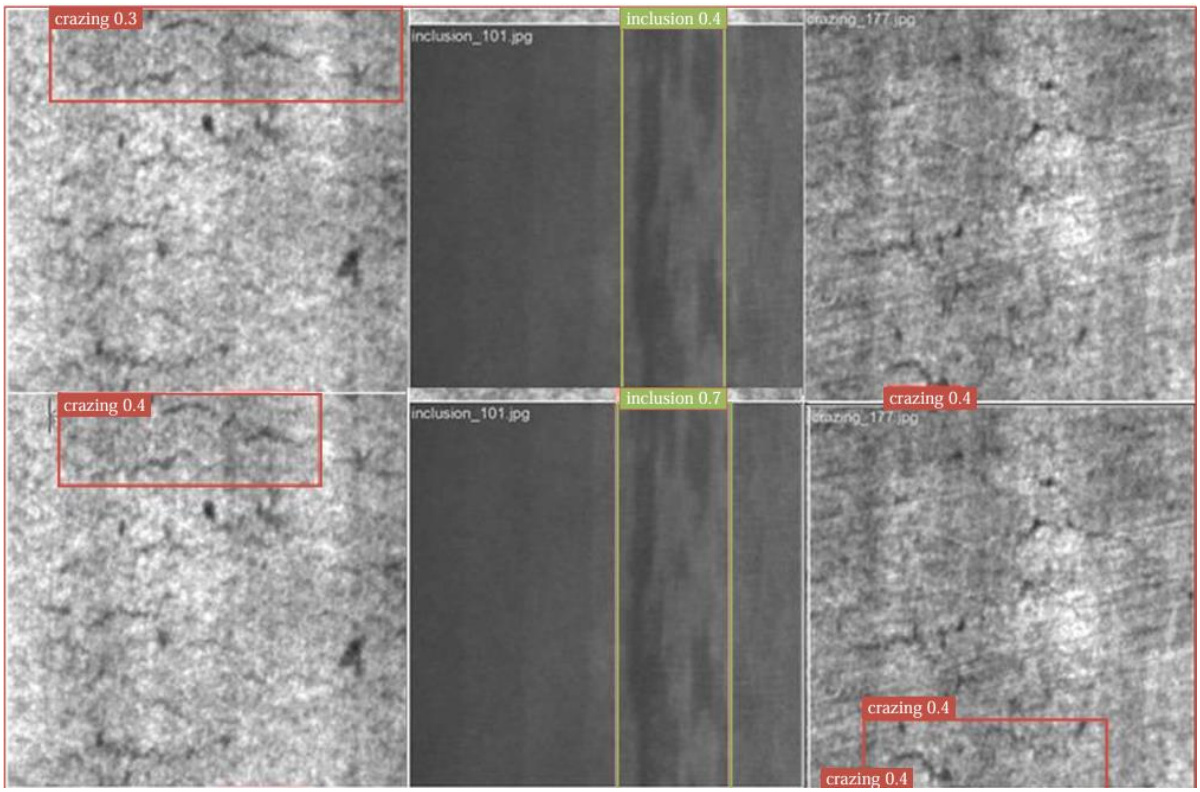

Fig. 12. The detection results on NEU-DET datasets

original baseline model and the bottom image is the test results of the improved model.

Upon scrutinizing Fig. 12, the improved network model has improved in various indicators. It demonstrates heightened accuracy and recall, resulting in increased confidence levels and, consequently, more effective overall detection performance. These enhanced capabilities also empower the model to better cater to metal surface defect detection and related domains. Moreover, the third set of images illustrates that the improved model effectively addresses crucial issues in metal defect detection, such as mitigating false negatives.

The robustness of the improved network model is further supported by detection results from diverse datasets, affirming its substantial progress and a commendable degree of applicability. By consistently demonstrating excellent performance across multiple data sets, the model enhances its reliability and applicability.

F. Ablation Experiment

To verify the improvement of the YOLOv8s model proposed in this paper, we conducted a series of experiments on the NEU-DET dataset to evaluate its performance The experimental results are presented in Table II. This paper introduces three enhancements to the YOLOv8s algorithm. To illustrate the beneficial effects of each module on the original algorithm, the following ablation experiments were conducted:

1. Solely integrating the CBAM attention mechanism into the model.
2. Exclusively replacing the SPPF module of the original algorithm with the SPPFCSPC module.
3. Adding a small target detection head solely to the end of the model's head.

Analysis of the table indicates a significant improvement in the enhanced network model compared to the original model, resulting in a notable 3.3% increase in mAP for the NEU-DET dataset. These findings suggest that with each modification, there is a rise in the network's mAP values, underscoring the efficacy of the proposed enhancements.

TABLE II
ABLATION EXPERIMENTS RESULTS ON NEU-DET DATASET

CBAM	HEAD	SPPFCSPC	mAP
×	×	×	67.1%
√	×	×	68.7%
×	√	×	68.2%
×	×	√	68.8%
√	√	×	69.1%
×	√	√	69.5%
√	×	√	69.9%
√	√	√	**70.4%**

G. Compared with Other Models

In order to verify the effectiveness of this method in the detection of steel surface defects, this paper tests the algorithm on the NEU-DET dataset. The evaluation entails comprehensive comparisons with algorithms including YOLOv5s, YOLOv7, Fast RCNN, YOLOv8, etc., across parameters such as mAP, floating-point operations per second (FLOP), inference speed, and other metrics. Detailed results are provided in Table III for reference.

Upon analyzing the data presented in Table III, it becomes apparent that our proposed model outperforms other algorithms significantly, excelling in both accuracy and inference speed.

Despite CMS-YOLOv8s having a larger parameter count than YOLOv8, it showcases a noteworthy 3.3% improvement in detection accuracy, accompanied by a substantial increase in inference speed. The experimental results suggest that even with a marginal increase in model parameters, the object recognition

capabilities and speed of the model may not necessarily be adversely affected. In comparison to other mainstream algorithms, such as Faster R-CNN and YOLOv5s, CMS-YOLOv8s also has significant advantages in terms of detection accuracy. These findings underscore the effectiveness and efficiency of our proposed model, positioning it as a robust solution in the realm of object detection algorithms.

TABLE III
COMPARED WITH OTHER MODELS

Model Name	mAP(%)	Inference(ms)	Flops(G)
YOLOv5s	66.1	5.8	23.8
Faster R-CNN	65.3	6.1	13.3
YOLOv7	63.9	15.3	35.3
YOLOv8	67.1	18.3	32.6
CMS-YOLOv8s	**70.4**	**23.2**	**37.2**

V. CONCLUSION

Building upon the YOLOv8s algorithm, this paper introduces an enhanced metal surface defect detection algorithm, referred to as CMS-YOLOv8s, which surpasses existing mainstream object detection algorithms. Key improvements include the integration of a lightweight attention mechanism CBAM, facilitating attention operations in both spatial and channel dimensions. This enhancement amplifies the model's emphasis on relevant information and enhances its feature extraction capabilities. Moreover, a small object detection head is integrated to enhance the model's ability to detect small targets, enabling the network to identify objects across different scales and thus improving overall detection effectiveness The introduction of the SPPFCSPC module expands the model's receptive field, fortifying its robustness and further amplifying its detection performance and resilience. Through this series of refinements, the proposed CMS-YOLOv8s algorithm makes significant strides in metal surface defect detection, notably enhancing accuracy, performance, and versatility.

REFERENCES

[1] C. D. Soukup and R. Huber-Mörk, "Convolutional neural networks for steel surface defect detection from photometric stereo images," *International Symposium on Visual Computing. Cham: Springer International Publishing*, pp. 668-677, 2014.

[2] J. Z. Chuande, L. Zhenyu, L. Zhongliang, "Metal surface defect detection based on improved YOLOv5," *Scientific Reports*, 2023.

[3] J. Q. Luo, X. Fang, L. Liu, "Automated visual defect detection for flat steel surface," *IEEE Transactions on Instrumentation and Measurement*, vol. 69, no.3, pp. 626-644, 2020.

[4] Tang, Bo, "Review of surface defect detection of steel products based on machine vision," *IET Image Processing*, pp. 303-322,2023.

[5] Y. He, K. Song, Q. Meng, "An end-to-end steel surface defect detection approach via fusing multiple hierarchical features," *IEEE Transactions on Instrumentation and Measurement*, vol. 69, no. 4, pp. 1493-1504,2019.

[6] J. B. Tang, L. Chen, W. Sun, "Review of surface defect detection of steel products based on machine vision," *IET Image Processing*, vol. 17, no. 2, pp. 303-322, 2023.

[7] C. Abu, M, "The performance analysis of transfer learning for steel defect detection by using deep learning," *Journal of Physics: Conference Series*, vol. 1755, no. 1, 2021.

[8] R. Usamentiaga, D. Lema, O. Pedrayes, "Automated surface defect detection in metals: A comparative review of object detection and semantic segmentation using deep learning," *IEEE Transactions on Industry Applications*, vol. 58, no.3, pp.4203-4213.

[9] Jiang, Peiyuan, "A Review of Yolo algorithm developments." *Procedia Computer Science*, pp. 1066-1073, 2022.

[10] J. T. Diwan, G. Anirudh, J. Tembhurne, "Object detection using YOLO: Challenges, architectural successors, datasets and applications," *Multimedia Tools and Applications*, vol. 82, no. 6, pp. 9243-9275, 2023.

[11] J. M. Hussain, "YOLO-v1 to YOLO-v8, the Rise of YOLO and Its Complementary Nature toward Digital Manufacturing and Industrial Defect Detection," *Machines*, vol. 11, no. 7, pp. 677, 2023.

[12] X. Zheng, S. Zheng, Y. Kong, "Recent advances in surface defect inspection of industrial products using deep learning techniques," T*he International Journal of Advanced Manufacturing Technology*, vol. 113, pp. 35-58, 2021.

[13] J. J. Li, Z. Su, J. Geng, "Real-time detection of steel strip surface defects based on improved yolo detection network," *IFAC-PapersOnLine*, vol. 51, no. 1, pp. 76-81, 2018.

[14] Y. Wang, H. Wang, "Efficient detection model of steel strip surface defects based on YOLO-V7," *IEEE Access*, vol. 10, pp. 133936-133944, 2022.

[15] Z. Guo, C. Wang, G. Yang, "Msft-yolo: Improved yolov5 based on the transformer for detecting defects of the steel surface," *Sensors*, vol. 22, no. 9, pp. 3467, 2022.

[16] L. Wang, X. Liu, J. Ma, "Real-Time Steel Surface Defect Detection with Improved Multi-Scale YOLO-v5," *Processes*, vol. 11, no. 5, pp. 1357, 2023.

[17] Y. Li, S. Xu, Z. Zhu, "EFC-YOLO: An Efficient Surface-Defect-Detection Algorithm for Steel Strips," *Sensors*, vol. 23, no. 17, pp. 7619, 2023.

[18] G. Wang, Y. Chen, P. An, "UAV-YOLOv8: a small-object-detection model based on improved YOLOv8 for UAV aerial photography scenarios," *Sensors*, vol 23, no.16, pp.7190, 2023.

[19] J. E. Scott, "SPPF-style parsing from Earley recognizers," *Electronic Notes in Theoretical Computer Science*, vol. 203, no. 2, pp. 53-67, 2008.

[20] J. H. Lou, X. Duan, J. Guo, "DC-YOLOv8: Small-Size Object Detection Algorithm Based on Camera Sensor," *Electronics*, vol. 12, no.10, pp. 2323,2023.

[21] C. S. Woo, J. Park, J. Lee, "Cbam: Convolutional block attention module," *Proceedings of the European Conference on Computer Vision (ECCV)*, 2018.

[22] Kuncham S.P., Harikrishnan P.K., Tapatee S., and Kedukodi B.S., "On Positive Cone and Partial Order in a Generalized Algebraic System," Engineering Letters, vol. 32, no. 1, pp136-142, 2024.

[23] Xiaoming Zhang, and Ying Tian, "Improved YOLOv5s Traffic Sign Detection," Engineering Letters, vol. 31, no.4, pp1883-1893, 2023.

[24] Siti Nurmaini, Alexander Edo Tondas, Radiyati Umi Partan, Muhammad Naufal Rachmatullah, Annisa Darmawahyuni, Firdaus Firdaus, Bambang Tutuko, Rachmat Hidayat, and Ade Iriani Sapitri, "Automated Detection of COVID-19 Infected Lesion on Computed Tomography Images Using Faster-RCNNs," Engineering Letters, vol. 28, no.4, pp1295-1301, 2020.